BEHAVIOR OF THERMAL SPRAY COATINGS AGAINST HYDROGEN ATTACK

Fabio Vargas*[1], Guillermo Latorre*[2] and Iván Uribe[1]

[1]Universidad Industrial de Santander, Escuela de Ingeniería Metalúrgica y Ciencia de Materiales
Grupo de Investigación en Corrosión
[2]Ecopetrol S.A. – ICP Instituto Colombiano del Petróleo, A.A. 4185 Bucaramanga, Santander, Colombia
e-mail: fabiovargas@citema.org.co e-mail: glatorre@ecopetrol.com.co

The behavior of nickel and chrome alloys applied as thermal spray coatings to be used as protection against embrittlement by hydrogen is studied.

Coatings were applied on a carbon steel substrate, under conditions that allow obtain different crystalline structures and porosity levels, in order to determine the effect of these variables on the hydrogen permeation kinetics and as a protection means against embrittlement caused this element.

In order to establish behaviors as barriers and protection, hydrogen permeation and corrosion tests under stress were carried out, supported by measurements of the potential's drop in the substrate-coating system under simultaneous conditions of stress and a corrosive agent with H_2S in solution.

Findings show that alloy coatings with face centered cubic structure possess greater hydrogen solubility than coatings with body centered cubic structures and than carbon steel used as substrate. Additionally, porosity inherent to the formation of this type of coating reduces hydrogen diffusion through its structure. The analysis of these results allows selecting the coating with better performance as a protection means against embrittlement by hydrogen.

* To whom correspondence may be addressed

S e estudia el comportamiento de aleaciones de níquel y cromo aplicadas como recubrimientos mediante termo-rociado, para ser utilizadas como protección ante la fragilización por hidrógeno.

Los recubrimientos fueron aplicados sobre un substrato de acero al carbono, bajo condiciones que permitieron obtener diferentes estructuras cristalinas y niveles de porosidad, con el fin de determinar el efecto de estas variables en la cinética de permeación de hidrógeno y como medio de protección ante la fragilización producida por este elemento.

Para establecer el comportamiento como barrera y protección, se realizaron pruebas de permeación de hidrógeno y de corrosión bajo esfuerzos apoyadas por mediciones de la caida de potencial del sistema substrato recubrimiento en condiciones simultáneas de esfuerzos de tensión y un agente corrosivo con H_2S en solución.

Se pudo establecer que los recubrimientos de aleaciones con estructura cristalina cúbica centrada en las caras poseen mayor solubilidad del hidrógeno, que los recubrimientos con estructura cúbica centrada en el cuerpo y que el acero al carbono utilizado como substrato. Adicionalmente, la porosidad propia de la conformación de este tipo de recubrimientos reduce la difusión de hidrógeno a través de su estructura. El análisis de estos resultados permitió seleccionar el recubrimiento de mejor desempeño como medio de protección ante la fragilización por hidrógeno.

Palabras claves: *fragilización por hidrógeno, recubrimientos termo-rociados, permeación de hidrógeno, corrosión bajo esfuerzos.*

INTRODUCTION

Damages caused by hydrogen on steel are a frequent problem in the oil industry and usually compromise operational integrity, especially of equipment used in hydrocarbon refinement, thus generating high maintenance costs.

Several equipment used in oil refinement process with H_2S in solution of up to 50 ppm or more, making it susceptible to Hydrogen-Induced-Cracking (HIC), Stress-Oriented Hydrogen Induced Cracking (SOHIC), Sulfur Stress Cracking (SSC), and blistering.

One of the most critical damages is induced cracking (HIC), produced in high resistance and low alloy steel, due to the absorption, trapping, and recombination of atomic hydrogen in the internal structure of the material (Dias, 1994; Fukai, 1993; Hirth, 1984). Such trapping might imply an increment in molecular hydrogen pressure that, together with the effects of tensions and discontinuities concentration on the steel structure, originate fragile cracking process such as that shown in Figure 1, where the morphology of the inter-granular damage induced by the presence of hydrogen in the structure of a component of the Barracabermeja refinery can be observed.

Costs involved in unscheduled stops, equipment repairs, potential risks for workers, and deterioration of the environment caused by HIC, justify the research
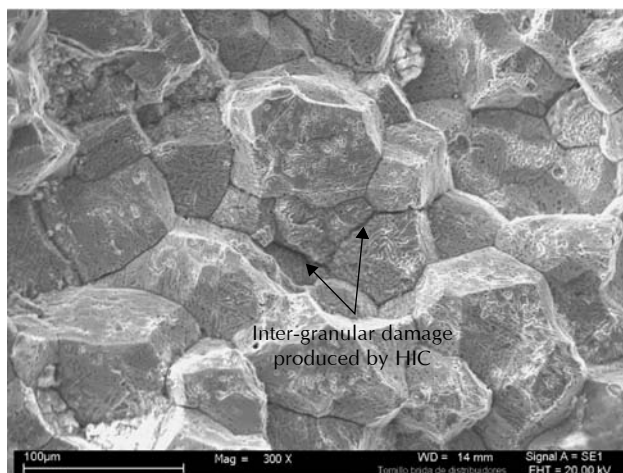
efforts carried out to understand the mechanisms inherent to the occurrence of this cracking phenomenon, to establish reliable lab tests that reproduce conditions at which this type of damage is produced, and to search for alternate solutions.

Application of alloy coatings resistant to cracking produced by hydrogen on metallic substrates of lower cost (for example, carbon steel) is a technically and economically favorable alternative for the solution of these problems. Thermal-spray is a relatively new technique that enables the application of coatings of diverse alloys to components and equipment of different geometries and sizes, both at plant and field levels.

Due to the characteristics inherent to the application process, thermal-spray coatings feature pores that, under certain conditions, may act as traps to stop hydrogen that has been able to enter the coating structure (Iwona and Karol, 1998; Herman and Sampath, 1996).

Nevertheless, it is important to emphasize that the final performance of the thermal-spray coatings used as a barrier to block the hydrogen path depend on the chemical composition of the material used as coating, its microstructure, its structural defects, and its capacity to keep its structural integrity under stress conditions to which it might be exposed during use.

EXPERIMENTAL DEVELOPEMENT

For the execution of these tests, samples were prepared through the application of alloy coatings with high contents of nickel and alloys with high contents of chrome, using combustion and electric arc techniques on carbon steel AISI 1010 substrates. The samples were coded according to the process performed, as shown in Table 1.

The coatings applied through combustion thermal spray used metallic powders heaters with a flame produced with a mixture of acetylene – oxygen, while the arc spray coatings was applied heating a metallic wire with electric arc.

Chemical characterization

The chemical composition of the alloys applied as coatings in samples R-1 and R-3 was determined by

Figure 1. Fragile fracture, produced by inter-granular cracking due to the presence of hydrogen in the metal's structure

Table 1. Sample code and its chemical composition

Sample Code	Application Technique	Chemical Composition
R – 1	Combustion	97,5 % Ni 2,04% Al 0,05% C
R – 2	Combustion	87,3 % Ni 4,7 % Cr 1,7 % Al 6,3 % Fe
R – 3	Electric Arc	1,5 % Ni 21,8 % Cr 3,8% Mn Balance Fe
S	--	0,09% C 0,4 % Mn Balance Fe

R = Coating applied to substrate
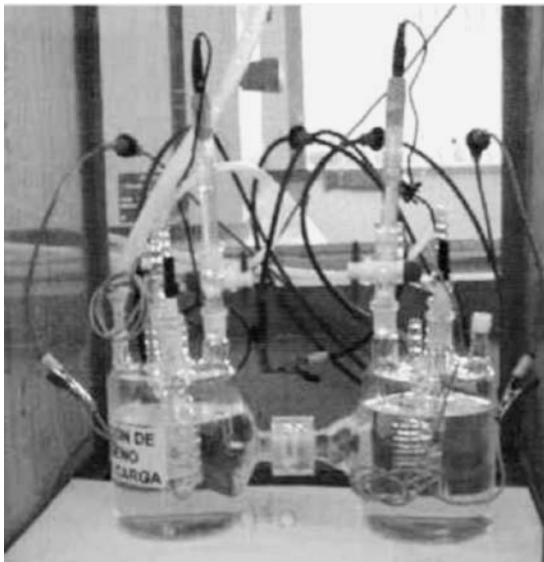S = Substrate without coating

Figure 2. Devanathan's cell used in hydrogen permeation tests

Optical Emission Spectrometry (OES). As for sample R-2, it was necessary to apply the Atomic Absorption (AA) technique, since verification patterns through spectrometry for this alloy are unavailable.

Structural and microstructural analysis

The analysis of the microstructure and defects on the applied coatings was carried out through optical microscopy, complemented with a digital image analysis

Table 2. Conditions test for the hydrogen permeation test

Parameter Test	Oxidation Cell	Load Cell
Electrolyte	NaOH 0,1 N	
Potential applied	0,345 volts Vs Ag/AgCl	-1,45 volts Vs Ag/AgCl
Temperature	297K	

sotfware to identify and quantify the presence of pores. The analysis was carried out on the transversal section of each of the applied coatings, revealing the phases present by chemical attack.

Hydrogen permeation

The kinetics study of hydrogen permeation in carbon steel samples coated with different alloys was carried out according to ASTM G148-97 standard, through Devanathan's duplo-potentiostatic technique, complemented by the methodology developed for the study of hydrogen permeation in coated substrates (Miranda and Fassini, 1993), which establishes that the current variation generated by hydrogen diffusion in the sample through time shall be measured both in the coated face and in the substrate facing the hydrogen generating environment in the charge cell.

As for experimental traceability, letters (RS) or (SR) are added to the samples to be evaluated, according to the arrangement of the samples in the test, in such a way that the (RS) code indicates that the sample was placed with the coated face facing the hydrogen generating environment in the charge cell. The (SR) code indicates that during the test, the substrate was placed with the substrate facing the hydrogen generating environment in the charge cell.

Figure 2 shows Devanathan's cell, as used to perform the hydrogen permeation tests. The test conditions under which the hydrogen permeation were carried out are shown in Table 2.

Corrosion under stress test

Corrosion test under stress test was performed according to the NACE TM 0177-96 standard, to evaluate the behavior of the studied coatings under simultaneous

conditions of tensile stress and highly hydrogenated corrosive environment.

Intended to be used as a corrosive medium, an aqueous solution of pH 2,99 was prepared with 5% in weight of NaCl, $1*10^{-3}$ mol/liter of hydrated sodium thiosulfate $Na_2S_2O_3$. 5 H_2O and 0,5% of acetic acid. This allows achieving a high content of H_2S, one of the main promoters of embrittlement by hydrogen. In the cell used to carry out this test, a potential of -600 mV was applied between the auxiliary platinum electrode and the sample test, to produce H_2S in solution through electrolysis.

To verify the integrity of the coating during the test and its effectiveness as a protection medium for the substrate against embrittlement by hydrogen, this was periodically monitored by means the potential drop technique, which, according to Tsai and Shih (1997), is adequate for such purpose. This test involves the application of a current of 500 mA to the sample immersed in the solution test and to a reference sample in air, and the measurement of the response voltage. The resistance of the sample may be calculated through Ohm's law.

Afterwards, the current is inverted to -500 mA and the new value for the resistance is calculated. Relative resistance for the sample in air and that of the test in the aqueous solution (with H_2S in solution) was calculated through the following expression (Tsai and Shih, 1997):

$$Rrel. = \frac{\left(\dfrac{R_+ + R_-}{2} \right)}{\left(\dfrac{R^0_+ + R^0_-}{2} \right)} \quad (1)$$

R_+ is the resistance of the sample in the corroding medium whenever a positive current is applied

R^0_+ is the resistance of the sample in air whenever a positive current is applied

A change in the system's relative resistance is an indicator of deterioration of the sample that acts as a conducting medium of the current fed into the circuit.

The tensile stress applied to each of the samples test was 80% of the elastic limit for the material used as substrate.

Effectiveness of the coatings studied as a protective medium against embrittlement by hydrogen was analyzed through the elongation suffered by the assayed sample prior to the fracture and through the relative resistance of the coating-substrate system.

RESULTS

Structural and microstructural analysis

Micro-structural and structural analysis carried out through optical microscopy to each one of the samples showed that coating R-1 features high contents of a nickel-rich phase, known as gamma prima (γ'), which has a face centered cubic structure, being one of the most compact structures to be found in metals. Figure 3.

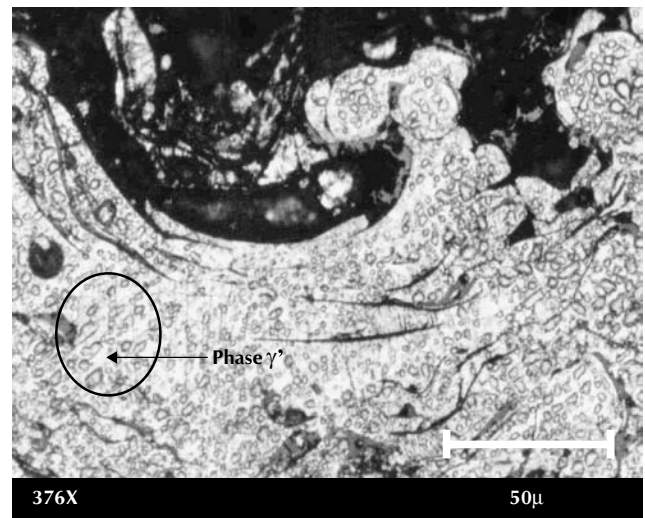Figure 3. R-1 coating microstructure, corresponding to phase γ'

Coating R-2 contains grains with combined phases corresponding to a gamma prima (γ') and fine martensite. Martensite possesses a body centered cubic structure, being one of the least compact structures to be found in metals. Figure 4.

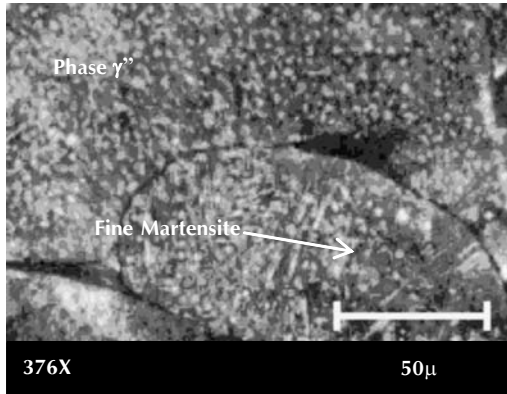Coating R-3 features a microstructure with high content of ferrical phase, with body centered cubic

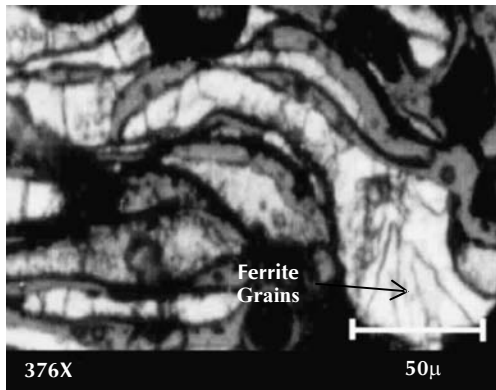Figure 4. R-2 coating microstructure, corresponding to combined grains of phase γ' and fine martensite

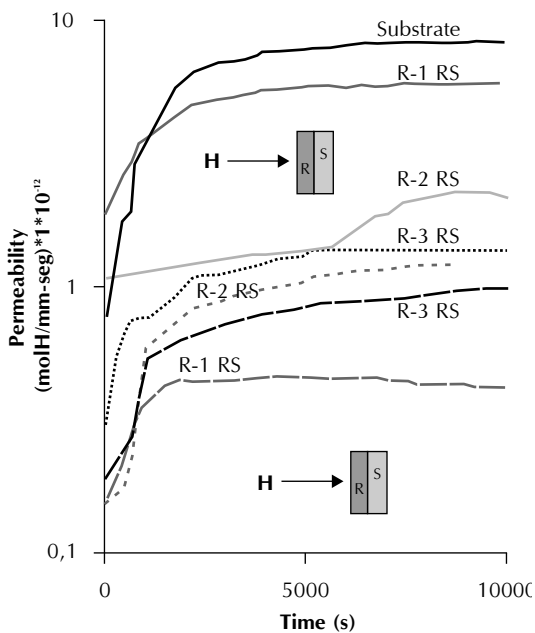Figure 5. R-3 coating microstructure. The arrow signals the ferrite grains. 376X

Figure 6. Results for the hydrogen permeation tests

structure, being one of the least compact structures to be found in metals. Figure 5.

The percentage of pores found in each of the samples analyzed was: R-1=18,96±1,4; R-2=5,27±0,74; R-3=7,43±0,6.

Hydrogen permeation

Each of the samples assayed presented different current variation, produced by hydrogen diffusion in the sample through time. Based on the results for each of the tests carried out, hydrogen permeation curves were constructed as shown in Figure 6.

To determine the influence of structural defects in the hydrogen permeation kinetics, each of the studied samples was subject to a second permeation test, in which the sample is set with the coated face facing the hydrogen generating environment in the charge cell.

Table 3 reports the parameters of the hydrogen permeation kinetics as calculated from the results obtained in the first and second hydrogen permeation carried out on the studied samples.

Corrosion under stress test

Each of the samples evaluated through the corrosion under stress test, showed a different elongation percentages prior to the fracture and different levels of coating deterioration through time.

The elongation percentage experimented by each sample prior to fracture and the time at which the fault occurred are reported in Table 4.

Results for the relative resistance produced by the coating's deterioration (break up) and calculated as the voltage measures found in the potential fall test, are shown in Table 5 and represented in Figure 7.

ANALYSIS AND DISCUSSION OF RESULTS

Hydrogen diffusivity calculated for each coating applied to the substrate, decrease as the percentage of pores that contain these coatings increases. See Table 6.

Table 6 shows that hydrogen diffusivity in carbon steel used as substrate is 328,81 times greater than the diffusivity of this element in sample R-1, which features

Table 3. Hydrogen-permeation kinetics parameters in coatings

Code	D (mm²/seg)	S (mol H/ mm³)	P (mol H/mm-seg)
Substrate	$1,529*10^{-5}$	$5,88*10^{-7}$	$7,98*10^{-12}$
R – 1	$4,65*10^{-8}$	$1,38*10^{-5}$	$6,43*10^{-13}$
R-1 (2 Perm.)	$4,65*10^{-8}$	$2,47*10^{-5}$	$1,14*10^{-12}$
R – 2	$5,13*10^{-7}$	$6,37*10^{-7}$	$3,27*10^{-13}$
R – 2 (2 Perm.)	$5,13*10^{-7}$	$7,82*10^{-7}$	$4,01*10^{-13}$
R - 3	$2,39*10^{-7}$	$1,55*10^{-6}$	$3,71*10^{-13}$
R – 3 (2 Perm.)	$2,39*10^{-7}$	$6,07*10^{-6}$	$1,45*10^{-12}$

D = Difusional coefficient
S = Solubility coefficient
P = Hydrogen permeation

Table 4. Results for the measurement of elongation percentage against time

Sample Code	% Elongation				
	Time (hours)				
	0	4	24	120	240
Substrate	0	Flaw	X	X	X
R – 1	0	0	0,05	0,075	0,075
R – 2	0	0	0,075	2	Flaw
R – 3	0	0	0,05	0,075	0,075

the largest content of pores and therefore, shows the lowest hydrogen diffusivity rating. Reduction in hydrogen diffusivity in coatings with a high content of pores may be attributed to the behavior of these empty spaces, acting as a proper site for the recombination of atomic hydrogen where molecules and hydrogen compounds may be formed, remaining trapped in these places.

Iwona and Karol (1998), established that coatings applied by thermal-spray may impede the effective diffusion of hydrogen through its structure, by trapping hydrogen atoms in interfaces or other structural imperfections in these type of coatings.

Hydrogen's greatest solubility was found in the coating of sample R-1, which features high precipitation of gamma prima γ' phase. This behavior may be attributed to the high solubility that hydrogen has in the face centered cubic structure, typical of this phase (Silva *et al.,* 1984).

Table 7 shows that hydrogen solubility in the face centered cubic structure in the coating of sample R-1 is 26,43 times greater than the solubility of this element in the body centered cubic structure of carbon steel used as substrate and 8,9 times greater than the one in the R-3 sample's coating.

Increases in hydrogen permeability during the second permeation of each coating applied to the substrate may be attributed to the partial or total filling with hydrogen of the pores or empty spaces in the coating
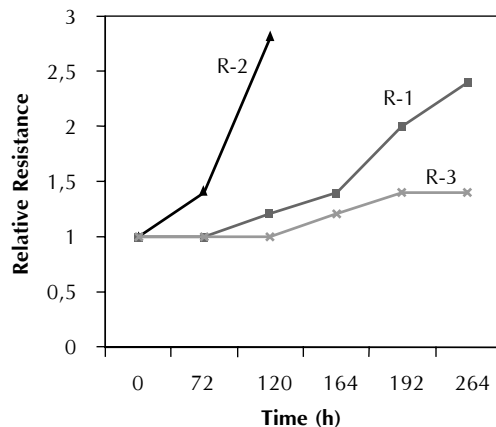

Figure 7. Relative resistance for the coated samples

Table 5. Results for the relative resistance of the
substrate-coating system

Sample Code	Relative Resistance					
	Time (hours)					
	0	72	120	164	192	264
Substrate	1	X	X	X	X	X
R-1	1	1	1,2	1,4	2	2,4
R-2	1	1,4	2,8	X	X	X
R-3	1	1	1	1,2	1,4	1,4

that during the first permeation probably acted as a hydrogen retention medium; therefore, during the second permeation, hydrogen that enters the coating structure goes through it with less difficulty, since part of the traps (pores) are filled with molecules or hydrogen compounds. Table 8 shows the difference between the first and second stages of hydrogen permeation for each sample.

During the corrosion under stress test, samples coated with alloys featuring high nickel contents (97, 5 % Ni; 87, 3% Ni) and high chrome contents (21,8% Cr), presented higher elongation ratings prior to fracture, as compared against the uncoated sample; therefore, protection given by these coatings to the substrate against the harmful effects of the H_2S contained in the Sodium

Table 6. Effect of the contents of the coating pores on
hydrogen diffusiveness

Sample Code	Diffusiveness (mm²/seg)	(%) of Pores	Correlation Factor (Kd)
Substrate	$1,529*10^{-5}$	0	328,81
R-1	$4,65*10^{-8}$	18,96	1
R-2	$5,13*10^{-7}$	5,27	11,03
R-3	$2,39*10^{-7}$	7,43	5,13

Correlation factor for diffusiveness among samples, taking as a reference diffusiveness of sample R-1 Dmuestra x = Kd *DR- 1

Table 8. Difference in hydrogen permeation between permeation
stages for each sample

Sample Code	Hydrogen Permeability (mol H/mm-seg)	
	First Stage	Second Stage
R-1	$6,43*10^{-13}$	$1,14*10^{-12}$
R-2	$3,27*10^{-13}$	$4,01*10^{-13}$
R-3	$3,71*10^{-13}$	$1,45*10^{-12}$

Thiosulfate solution, retards nucleation and unstable propagation of cracks.

Failure by the sample coated with coating R-2 after 240 hours of test is probably due to the synergy caused by the tensile stress applied to the sample test and to embrittlement by hydrogen that the martensitical particles may suffer.

Coating R-1 sample shows a high tendency to grow in relative resistance through time, indicating progressive deterioration of this coating. This deterioration is caused by the combined effect of possible blistering in the layer's interior and the tensile stress applied during the test.

Blistering in thermal-sprayed coatings is generally due to excessive retention and recombination of hydrogen inside the pores or empty spaces.

Table 7. Effect of the coating's crystalline structure on
hydrogen solubility

Simple Code	Solubility (mol H/mm³)	Crystalline Structure	Correlation Factor (Ks)
Substrate	$5,22*10^{-7}$	BCC	1
R-1	$1,38*10^{-5}$	FCC	26,43
R-2	$6,37*10^{-7}$	BCC–FCC	1,22
R-3	$1,55*10^{-6}$	BCC	2,96

Calculated factor. To establish the correlation between the solubility of different samples, this factor was calculated while taking the substrate's solubility as reference. S_{sample} x = Ks *$S_{substrate}$

CONCLUSIONS

- Coatings with alloys featuring high contents of nickel and chrome, as applied by thermal-spray, act effectively as protection against embrittlement by hydrogen; however, the contents of pores from this type of coating may compromise its performance, due to excessive trapping and hydrogen recombination that may occur inside the pores.

- The pores contained in thermal-sprayed coatings act as appropriate places for the retention or entrapment of hydrogen, where this element may be recombined to form molecules and compounds, thus increasing its solubility in the coating structure.

- Protection capacity against embrittlement by hydrogen in coatings with martensitic phase, such as coating R-2, may be compromised by the synergic effect of mechanical stress and hydrogen embrittlement.

- Coatings with high contents of chrome preserve their ability to stop the advance of hydrogen and its structural integrity, even through high-tensile stress applications, thus allowing its usage as protection system against embrittlement by hydrogen under high concentration of hydrogen and tension stress, inasmuch as these do not exceed the cohesive resistance of the coating and the adherence to the substrate upon which it is applied.

- Coatings applied through the thermal spray method result in a very good protection alternative for structures and equipment in petrochemical plants against hydrogen attacks.

KNOWLEDGEMENTS

BIBLIOGRAPHY

Dias, M. F. D., 1994. *"Estudo dos efeitos da fragilizaçao pelo hidrogênio nos aços UNS – G41300E UNS – S 31803 através de ensaios de traçao com baixa taxa de deformaçao en soluçoes de tiossulfato de sodio"*. Universidade Federal Do Rio de Janeiro.

Fukai, Y., 1993. *"The metals hydrogen system"*. Springer-Verlag, New York.

Herman, H. and Sampath, S., 1996. *"Thermal spray coatings"*. In: Stern, K. H., Ed., Metallurgical and Protective Coatings, 1 Ed., Chapter 10, New York, Chapman & Hall.

Hirth, J. P., 1984. "Thories of hydrogen induced cracking of steels". *Hydrogen Embrittlement and Stress Corrosion Cracking,* A.M.S., Editorial R. Gibala y R. F. Hehemann, 29-4.

Iwona, S. O. and Karol, E. S., 1998. "Developing a methodology for performance evaluation of metallic thermal spray coating for oil and gas industry service". *Materials Performance,* July, 37 (7): 34-40.

Miranda, P. E. and Fassini F. D., 1993. "New methodology for the determination of hydrogen permeation parameters in layered materials". *J. Mater. Scien.,* 28: 5148-5154.

Miranda, P. E., 1984. "Hydrogen induced surface effects on the mechanical properties of type 304 stainless steel". *In: Fracture Prevention in Energy and Transport Systems,* Le May e S. N., Monteiro ed., London, EMAS, 511-520.

Silva, T. C., Pascual, R. and Miranda, P. E., 1984. "Hydrogen induced surface effects on the mechanical properties of type 304 stainless steel ". In: *Fracture Prevention in Energy and Transport Systems,* Le May e S. N. Monteiro ed., London, EMAS, 511-520.

Tsai, S. Y. and Shih, H. C., 1997. "The use of thermal spray coatings for preventing wet H_2S cracking in HSLA steels plates". *Corrosion Prevention and Control,* 42-48.